TIGIT Expression Is Associated with T-cell Suppression and Exhaustion and Predicts Clinical Outcome and Anti–PD-1 Response in Follicular Lymphoma

Zhi-Zhang Yang[1], Hyo Jin Kim[1], Hongyan Wu[2], Shahrzad Jalali[1], Xinyi Tang[1], Jordan E. Krull[1], Wei Ding[1], Anne J. Novak[1], and Stephen M. Ansell[1]

ABSTRACT

Purpose: T-cell immunoglobulin and ITIM domain (TIGIT), a member of the immune checkpoint family, is important in normal T-cell biology. However, the phenotypical profile and clinical relevance of TIGIT in follicular lymphoma is largely unknown.

Experimental Design: Biopsy specimens from a cohort of 82 patients with follicular lymphoma were analyzed using mass cytometry to explore the phenotype and biological and clinical significance of TIGIT$^+$ T cells.

Results: TIGIT is highly expressed on intratumoral T cells and its expression alters T-cell phenotype in follicular lymphoma. TIGIT is abundantly expressed on T_{reg} cells, resulting in an enhanced suppressive property. TIGIT expression on non-T_{reg}/T_{FH} T cells defines a population that exhibits an exhausted phenotype. Clinically, increased numbers of TIGIT$^+$ T cells are associated with inferior patient outcomes and poor survival. We observe that anti–PD-1 therapy with pembrolizumab alters the phenotype of TIGIT$^+$ T subsets and identifies a role for CD28 expression on TIGIT$^+$ T cells in treatment response.

Conclusions: The current study provides a comprehensive analysis of the phenotypic profile of intratumoral TIGIT$^+$ T subsets and their prognostic relevance in follicular lymphoma. Inhibition of TIGIT signaling may be an additional mechanism to prevent T-cell suppression and exhaustion in B-cell lymphoma.

Introduction

Immune checkpoint receptors are members of inhibitory receptors that play a critical role in regulating T-cell function. Although activation is essential for T-cell function, overactivation of T cells can be harmful by promoting an autoimmune response. Expression of immune checkpoint receptors provides physiologic inhibitory mechanisms for activated T cells to prevent an excessive immune response. However, under pathologic conditions such as cancer, suppression of T-cell function due to signaling via immune checkpoint receptors inhibits the immune response and results in insufficient tumor-directed cytotoxicity.

T-cell immunoglobulin and ITIM domain (TIGIT) was initially identified as a surface protein specifically on T and natural killer (NK) cells (1–3). Among T populations, TIGIT is mainly expressed by memory, activated T cells, and T_{reg} cells (1). It has been shown that TIGIT delivers an inhibitory signal to T cells, in which T cells lacking TIGIT expression had increased function when compared with T cells with TIGIT expression (4). CD155, a poliovirus receptor, is identified as the primary ligand for TIGIT (1, 5) and the ligation of CD155 and TIGIT delivers an inhibitory signal and suppresses T-cell function.

In cancer, TIGIT expression is upregulated on tumor-infiltrating lymphocytes (TIL) and the number of TIGIT-expressing T cells is commonly increased in the tumor microenvironment (6–8). TIGIT blockade restores T-cell function and elicits tumor rejection (8), suggesting that TIGIT signaling negatively regulates antitumor immunity. In hematologic malignancies, it has been found that TIGIT expression is upregulated on T cells from acute myelogenous leukemia (AML; ref. 9), chronic lymphocytic leukemia (10), and Sezary syndrome (11). Furthermore, increased numbers of TIGIT-expressing T cells are associated with disease relapse and progression in AML (9) and multiple myeloma (12). TIGIT$^+$ T cells from the tumor microenvironment usually display an exhausted phenotype as these TILs coexpress PD-1, TIM-3, and LAG-3 and exhibit reduced T-cell function (7, 13).

The biological role of TIGIT in follicular lymphoma has been explored in previous studies (14, 15). However, the expression of TIGIT has been assessed in broad terms with little known about TIGIT expression on specific intratumoral T-cell subsets, the phenotype of these TIGIT-expressing subsets, and the clinical relevance of TIGIT expression in follicular lymphoma. In the current study, we studied a large cohort of follicular lymphoma biopsy specimens (82 patients) with long clinical follow-up, and employed mass cytometry (CyTOF) to analyze TIGIT-expressing T cells in this cohort. We phenotypically characterized the TIGIT$^+$ T subsets, assessed the role of TIGIT in the function of these subsets, and measured whether TIGIT$^+$ T cells had an impact on patient outcome.

Materials and Methods

Patient samples

Patients providing written informed consent were eligible for this study if they had a tissue biopsy that on pathologic review showed follicular B-cell non-Hodgkin lymphoma (NHL) and adequate tissue to perform the experiments. Tonsils removed for nonmalignant reasons were used as controls. The use of human tissue samples for

[1]Division of Hematology and Internal Medicine, Mayo Clinic, Rochester, Minnesota. [2]Department of Immunology, Medical College, China Three Gorges University, Yichang, Hubei, China.

Note: Supplementary data for this article are available at Clinical Cancer Research Online (http://clincancerres.aacrjournals.org/).

Corresponding Authors: Zhi-Zhang Yang, Mayo Clinic, 200 First St SW, Rochester, MN 55905. Phone: 507-266-2161; Fax: 507-266-9277; E-mail: yang.zhizhang@mayo.edu; and Stephen M. Ansell, ansell.stephen@mayo.edu

Clin Cancer Res 2020;26:5217–31

doi: 10.1158/1078-0432.CCR-20-0558

Translational Relevance

As a member of the immune checkpoint family, T-cell immunoglobulin and ITIM domain (TIGIT) delivers an inhibitory signal to T cells. In this study, we confirm the role of TIGIT in T-cell suppression and exhaustion, and establish its importance in predicting clinical outcome in patients with follicular lymphoma. We show that when patients with follicular lymphoma are treated with PD-1 blockade, responding patients are those who have specific $TIGIT^+$ T-cell subsets that coexpress adequate levels of CD28. These findings not only support the therapeutic potential of targeting TIGIT in follicular lymphoma, but also may identify patients with a great potential for responding to immune checkpoint blockade.

this study was approved by the Institutional Review Board of the Mayo Clinic/Mayo Foundation. The study was conducted in accordance with the Declaration of Helsinki. Patient characteristics are summarized in Supplementary Table S1. Briefly, most patients in this cohort had follicular lymphoma grade 1/2 and were stage III and IV at diagnosis. The patients received various regimens as first-line treatment including rituximab alone, CHOP (cyclophosphamide, doxorubicin, vincristine, and prednisone) ± rituximab, CVP (cyclophosphamide, vincristine, and prednisone) ± rituximab, or chlorambucil. Most patients had either a complete or partial response after first-line treatment.

Flow cytometry and intracellular cytokine staining

Fresh tissues were minced into small fragments by using mechanical dissection of the tissues with a scalpel. Tissue samples were then filtered through a 60-μm strainer to make single-cell suspensions. Mononuclear cells (MNC) from tissues or peripheral blood (PB) were isolated by Ficoll–Hypaque density gradient centrifugation. MNCs from tissues or PB were lysed with ACK buffer to remove erythrocytes. $CD3^+$, $CD4^+$, and $CD8^+$ T cells were isolated using Human CD3, CD4, and CD8 Kits (STEMCELL Technologies), respectively. Cells were then stained with fluorochrome-conjugated Abs against TIGIT, PD-1, and TIM-3 for 30 minutes and analyzed by FACSCanto II flow cytometer (Becton Dickinson). For intracellular cytokine staining, cells were stimulated with phorbol myristate acetate and ionomycin (Ion) in the presence of protein transport inhibitor brefeldin A for 4 hours. After fixation and permeabilization, cells were stained with fluorochrome-conjugated antibodies for IL2, IFNγ, IL4, or TNFα plus surface marker antibodies for CD4, TIM-3, or CXCR5 in each specimen. Cells were then analyzed on a flow cytometer.

CFSE labeling and T-cell proliferation assay

Cells were washed, counted, and resuspended in PBS. A stock solution of CFSE (carboxyfluorescein succinimidyl ester; 5 mmol/L) was diluted 1:100 with PBS and added to the cells for a final concentration of 5 μmol/L. After 10 minutes at 37°C, cells were washed 3 times with 10 vol PBS containing 10% FBS. CFSE-labeled responding cells were cultured in anti-CD3 Ab-coated plates in the presence of anti-CD28 Ab at 37°C and 5% CO_2. Cells were harvested at day 3 and analyzed by flow cytometry. The percentage of $CFSE^{dim}$ were measured and calculated as the percentage of proliferated cells. For the proliferation assay, $TIGIT^+$ or $TIGIT^-$ T cells were isolated by flow cytometry. Cells were stained with CFSE 500 nmol/L for 10 minutes at room temperature and quenched with 10% FBS medium. For the inhibition assay, $CD4^+CD25^+TIGIT^+$ or $TIGIT^-$ T cells were cocultured with $CD8^+$ T cells. At day 5, CFSE intensity was measured by flow cytometry.

CyTOF

CyTOF was performed and analyzed as described previously (16). Cells were stained with a cocktail containing 37 metal-tagged mAbs designed to interrogate T-cell subpopulations. Two nucleic acid intercalator probes tagged with iridium (191Ir and 193Ir) were used to identify cellular events. Cisplatin (195Pt) was used as a viability marker. All affinity products tagged to metal isotopes were obtained from Fluidigm. Specimens were processed in batches to minimize variability and acquired on the CyTOF2 mass cytometer (Fluidigm). EQ Four Element Calibration Beads (Fluidigm) were used for instrument normalization.

CyTOF data analysis

The CyTOF data were analyzed using online software (Cytobank) as described previously (17, 18). All the samples were normalized and analyzed simultaneously to account for variability in signal across long acquisition times. A high-level gating strategy was applied simultaneously to all CyTOF files. For specific analysis purposes, we concatenated all sample files to one file. To generate flow files for certain population, we split files by the population and downloaded them into individual files for each sample. Linage markers (CD4, CD8, CD25, CD127, PD-1, CXCR5, CCR7, or CD45RO) were included in the analysis to identify T cells, and then distinguish T_{reg} cells, exhausted cells, naïve, or memory T cells.

A t-distribution stochastic neighbor embedding (tSNE) map was generated by the tSNE analysis that makes a pairwise comparison of cellular phenotypes to optimally plot similar cells close to each other and reduces multiple parameters into two dimensions (tSNE1 and tSNE2). For most analysis, we selected equal events for each sample. Channel (markers) selection was variable depending on cell populations to be clustered. We chose 3,000 iterations, perplexity of 30 or 50 and theta of 0.5 as standard tSNE parameters.

For SPADE analysis, we used 100 target numbers of nodes and 10% downsampled events target. The clustering channels were selected on the basis of which cell population to be clustered.

For CITRUS (cluster identification, characterization, and regression) analysis, models of significance analysis of microarrays and nearest shrunken centroid were selected for association analysis. Abundance was chosen for the cluster characterization and the minimal cluster size was 2%.

Statistical analysis

Statistical analysis was performed using the Student *t* test. Significance was determined at $P < 0.05$. For nonparametric data, a Mann–Whitney test or Wilcox matched-pairs rank test was performed. Overall survival (OS) or event-free survival (EFS) was measured from the date of diagnosis until death from any cause or until the date of next treatment, respectively. OS or EFS of all patients was estimated using the Kaplan–Meier method. The univariate associations between individual clinical features and survival were determined with the log-rank test. EFS24 (EFS at 24 months) achieved or failed was defined as patients who remained in remission or progressed within 24 months of diagnosis. Statistical analysis was performed using software GraphPad Prism 8 and JMP 14.

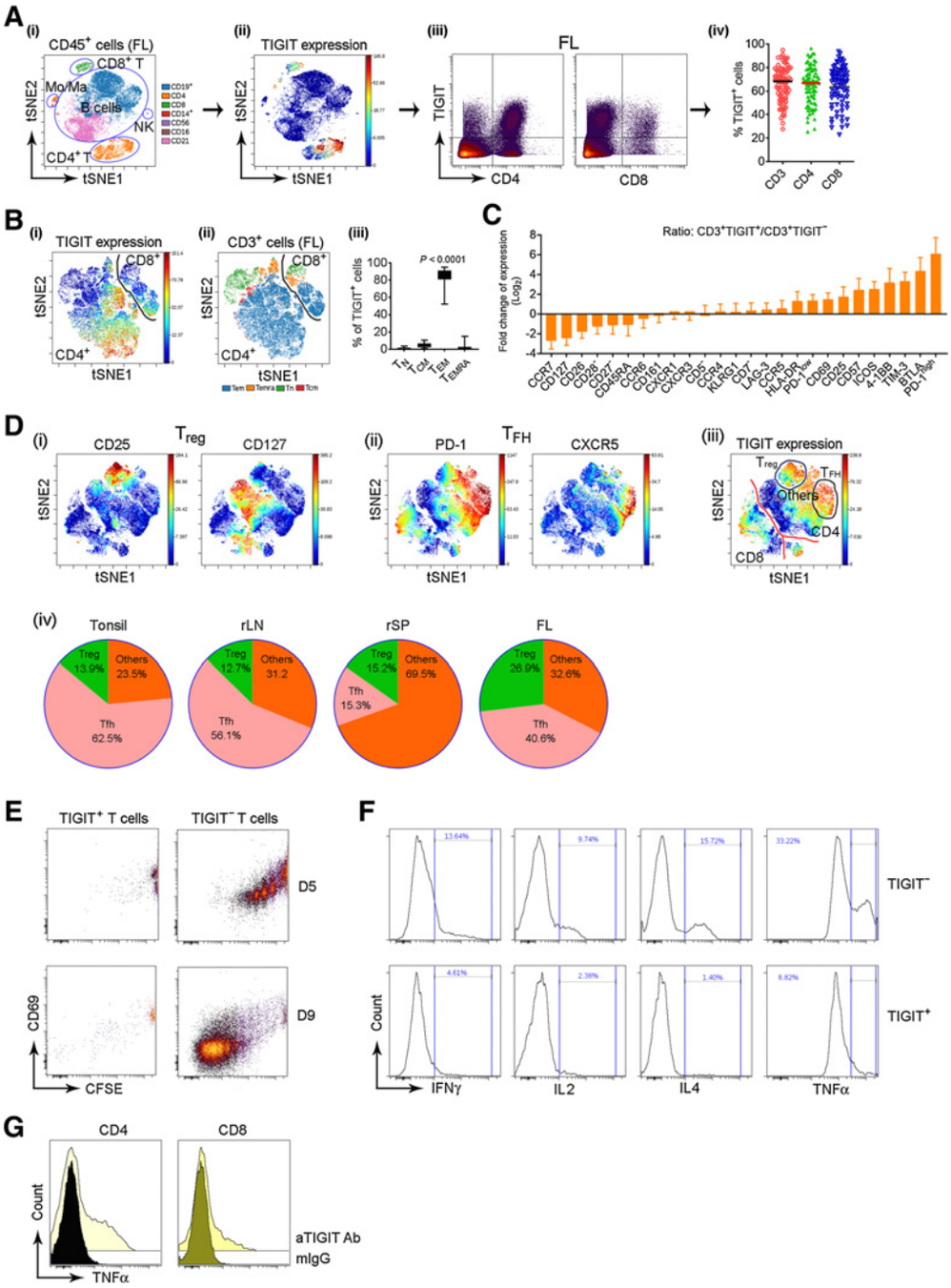

Figure 1.

TIGIT is abundantly and broadly expressed on subsets of intratumoral T cells in follicular lymphoma. **A,** The viSNE plot of $CD45^+$ cells from follicular lymphoma showing distribution of cell subsets (i) and TIGIT expression on these cell subsets (ii). Dot plots showing TIGIT expression on intratumoral $CD4^+$ or $CD8^+$ T cells from follicular lymphoma (iii). Graph showing percentage of $TIGIT^+$ cells in $CD3^+$, $CD4^+$, or $CD8^+$ T-cell population. $n = 82$ (iv). **B,** The viSNE plot of $CD3^+$ cells from follicular lymphoma showing distribution of T_N, T_{cM}, T_{EM}, and T_{EMRA} subsets (i) and TIGIT expression on these cell subsets (ii). Graph showing percentage of $TIGIT^+$ cells in T_N, T_{cM}, T_{EM}, and T_{EMRA} cell population. $n = 82$ (iii). **C,** Graph showing fold change (log_2) of surface marker expression in $TIGIT^+$ versus $TIGIT^-$ $CD3^+$ cells. **D,** The viSNE plots showing expression of CD25 and CD127 (i) to define T_{reg} cells (iii) or expression of PD-1 and CXCR5 (ii) to define T_{FH} cells (iii). The pie charts showing percentage of T_{reg}, T_{FH}, and non-T_{reg}/T_{FH} (others) in $CD4^+$ T cells from tonsil ($n = 6$), reactive lymph nodes ($n = 3$), reactive spleen ($n = 4$), and follicular lymphoma ($n = 31$; iv). **E,** Dot plots showing cell proliferation by CFSE staining of $TIGIT^+$ or $TIGIT^-$ T cells isolated by flow cytometer. Cells were cultured in an anti-CD3 Ab-coated plate in the presence of anti-CD28 Ab and harvested on day 5 and 9 for detection. **F,** Histograms showing cytokine expression by $TIGIT^+$ or $TIGIT^-$ $CD4^+$ cells. Expression of IFNγ, IL2, IL4, and TNFα was measured by intracellular staining. **G,** Histograms showing TNFα expression by $CD4^+$ or $CD8^+$ T cells after treatment with an anti-TIGIT blocking antibody or a control antibody. Expression of TNFα was measured by intracellular staining.

Results

TIGIT is abundantly and broadly expressed on subsets of intratumoral T cells in follicular lymphoma

To explore the biological and clinical relevance of TIGIT in follicular lymphoma, we first determined TIGIT expression in biopsy specimens of follicular lymphoma using both flow cytometry and CyTOF. T cells from tonsil tissue were used as a control. As shown in **Fig. 1A** and Supplementary Fig. S1A, TIGIT was abundantly expressed on intratumoral $CD3^+$ T cells, but virtually absent on resting T cells from peripheral blood of healthy donors, although stimulation with anti-CD3/CD28 Abs induced TIGIT expression in a time-dependent manner (Supplementary Fig. S1B). As a control, CD226, a receptor that shares ligands with TIGIT and competes for ligand binding was constitutively expressed on resting T cells from both peripheral blood and biopsy specimens of lymphoma (Supplementary Fig. S1B). $CD16^+$ or $CD56^+$ NK cells expressed low levels of TIGIT but the numbers of $CD16^+$ or $CD56^+$ cells were low in the follicular lymphoma biopsy specimens. $CD19^+$ B cells and $CD14^+$ monocytes lacked TIGIT expression (Supplementary Fig. S1A). Within the $CD3^+$ T-cell population, both $CD4^+$ and $CD8^+$ T cells expressed TIGIT (**Fig. 1A**, iii). In follicular lymphoma specimens, approximately 65.9% (range, 27.7%–94.8%, $n = 82$) of $CD3^+$, 64.8% (25.4%–96.3%, $n = 82$) of $CD4^+$, or 64.3% (22.9%–93.7%, $n = 82$) of $CD8^+$ T cells express TIGIT (**Fig. 1A**, iv). As shown in **Fig. 1B**, TIGIT-expressing $CD4^+$ and $CD8^+$ T cells were predominantly memory-type cells as the vast majority of $TIGIT^+$ cells (red, **Fig. 1B**, i) clustered with T_{EM} ($CD45RO^+CCR7^-$) cells (blue, **Fig. 1B**, ii). $CD3^+$ T_{EM} accounted for approximately 82% of $TIGIT^+$ T cells in follicular lymphoma while naïve, central memory, and terminally differentiated T cells displayed minimal expression of TIGIT (**Fig. 1B**, iii). When comparing with $TIGIT^-$ cells, $TIGIT^+$ T cells displayed increased expression of inhibitory receptors PD-1, TIM-3, LAG-3, BTLA, and ICOS, suggesting an exhaustion phenotype (**Fig. 1C**). Of note, a unique population of $TIGIT^+$ T cells were identified that lacked coexpression of immunoreceptors PD-1, TIM-3, LAG-3, BTLA, ICOS, and CD25 and accounted for approximately 9.04% (range, 1.38%–38.5%, $n = 82$) of all $TIGIT^+$ T cells (Supplementary Fig. S1C).

It appeared that TIGIT was abundantly expressed on T_{reg} ($CD4^+CD25^+CD127^-$) and T_{FH} ($PD\text{-}1^{high}CXCR5^+$) cells and other $CD4^+$ T cells (non-T_{reg}/T_{FH}; **Fig. 1D**). In follicular lymphoma specimens, T_{reg}, T_{FH}, and non-T_{reg}/T_{FH} cells accounted for 26.9%, 40.6%, and 32.6% of $TIGIT^+CD4^+$ cells, respectively (**Fig. 1D**, iv). In normal tonsil, more T_{FH} and fewer T_{reg} cells constituted the $TIGIT^+CD4^+$ population as $TIGIT^+$ T cells consisted of approximately 62.5% of T_{FH} and 13.9% of T_{reg} cells. These results suggest that $TIGIT^+$ T cells are heterogeneous and a variety of T subsets express TIGIT.

$TIGIT^+$ T cells showed reduced capacity for proliferation and cytokine production. As shown in **Fig. 1E**, the proliferation of $TIGIT^+$ cells by CFSE was virtually absent, while $TIGIT^-$ T cells retained their proliferative capacity when stimulated with anti-CD3 and anti-CD28 Abs. Similarly, the capacity of $TIGIT^+$ T cells for cytokine production was substantially reduced when compared with $TIGIT^-$ T cells (**Fig. 1F**). Supporting this, inhibition of TIGIT signaling using a blocking Ab enhanced TNFα expression by both $CD4^+$ and $CD8^+$ T cells (**Fig. 1G**).

TIGIT is expressed on activated T_{reg} cells with enhanced suppressive properties

As noted before, CD25 expression was frequently observed on a subset of $TIGIT^+$ T cells and less commonly seen in $TIGIT^-$ T cells (**Fig. 2A**). Approximately 78.1% (range, 37.7%–95.9%, $n = 31$) of $CD4^+CD25^+$ T cells expressed TIGIT, which accounted for approximately 26.9% (range, 5.9%–52.3%, $n = 31$) of the total $CD4^+TIGIT^+$ T cells (**Fig. 2A**). A small proportion (21.9%; range, 4.0%–62.3%, $n = 31$) of $CD4^+CD25^+$ T cells lacked TIGIT expression. The observation that Foxp3 was induced in $CD4^+TIGIT^+$ cells but not in $CD4^+TIGIT^-$ T cells supports the notion that TIGIT is preferentially expressed on T_{reg} cells (**Fig. 2B**).

Two T_{reg} subsets, namely resting and activated T_{reg} cells (rT_{reg} and aT_{reg}), are defined by coexpression of CD45RA and CD25 (rT_{reg}: $CD45RA^+CD25^{low}$; aT_{reg}: $CD45RA^-CD25^{high}$; refs. 19, 20). Although the majority of T_{reg} cells are aT_{reg} cells, a small portion of rT_{reg} cells exists in follicular lymphoma. rT_{reg} and aT_{reg} accounted for 2.5% and 17% of the total $CD4^+$ cells in follicular lymphoma, respectively (**Fig. 2C**). Control benign tissues such as reactive LN or SP had significantly higher rT_{reg} cells when compared with follicular lymphoma tumor tissue (**Fig. 2C**). We observed that the number of cells expressing TIGIT was significantly higher in the aT_{reg} than the rT_{reg} subset, and aT_{reg} cells tended to express higher levels of TIGIT when compared with rT_{reg} cells (**Fig. 2D**). Phenotypically, $CD25^+TIGIT^+$ T cells were distinct from $CD25^+TIGIT^-$ T cells (**Fig. 2E** and **F**). As shown in **Fig. 2F**, expression of CD27, CD28, and 4-1BB was significantly higher in $CD25^+TIGIT^+$ cells, suggesting that loss of costimulatory molecules was uncommon in $CD25^+TIGIT^+$ T cells when compared with $CD25^+TIGIT^-$ T cells. In addition, $CD25^+TIGIT^+$ T cells tended to be more activated, as the activation marker CD69 was highly expressed on $CD25^+TIGIT^+$ T cells when compared with $CD25^+TIGIT^-$ T cells.

T_{reg} subsets defined by TIGIT expression showed functional relevance as the suppressive capacity of $CD4^+CD25^+TIGIT^-$ cells and $CD4^+CD25^+TIGIT^+$ cells differed. As shown in **Fig. 2G**, although $CD4^+CD25^+TIGIT^-$ T cells suppressed the activation (CD25 expression) and proliferation (decreased CFSE expression) of $CD8^+$ T cells, this inhibitory effect was greater when $CD8^+$ cells were cocultured with $CD4^+CD25^+TIGIT^+$ cells. These results suggest that TIGIT plays a role in delineating specific subsets of T_{reg} cells with different suppressive capabilities.

TIGIT expression defines intratumoral non-T_{reg}/T_{FH} $CD4^+$ cells as exhausted cells

In addition to abundant expression of TIGIT on T_{reg} and T_{FH} cells, other $CD4^+$ T cells (non-T_{reg}/T_{FH}) also expressed TIGIT (**Fig. 3A**), but to a lesser extent when compared to T_{reg} and T_{FH} cells (**Fig. 3B**). Compared with $TIGIT^-$ T cells, non-T_{reg}/T_{FH} $TIGIT^+CD4^+$ population showed reduced expression of CD45RA, CCR7, and CD127, suggesting a more memory type-like T cell (**Fig. 3C**). The non-T_{reg}/T_{FH} $TIGIT^+CD4^+$ population displayed increased expression of inhibitory receptors PD-1, TIM-3, LAG-3, BTLA, and ICOS when compared with the $TIGIT^-CD4^+$ population, suggesting an immune exhaustion phenotype (**Fig. 3C** and **D**).

We then assessed the profile of T helper (T_H) cells in this population of non-T_{reg}/T_{FH} $TIGIT^+CD4^+$ cells. We identified T_H1, T_H2, T_H17, and T_H22 based on expression of CCR4, CXCR3, CCR5, CCR6, and CD161 and the gating strategy to define T_H subsets is presented in Supplementary Fig. S2. In follicular lymphoma, T_H1 cells dominated these T_H subsets, whereas other T_H subsets constituted minor populations. Approximately 38.7%, 9.7%, 7.2%, and 5.4% of the residual $CD4^+$ population were T_H1, T_H2, T_H17, and T_H22 cells, respectively (**Fig. 3E**). Compared with $TIGIT^-$ T cells, non-T_{reg}/T_{FH} $TIGIT^+$ T cells comprised a majority of the T_H1 cell population. We did not see a difference in the number of T_H2, T_H17, or T_H22 cells between

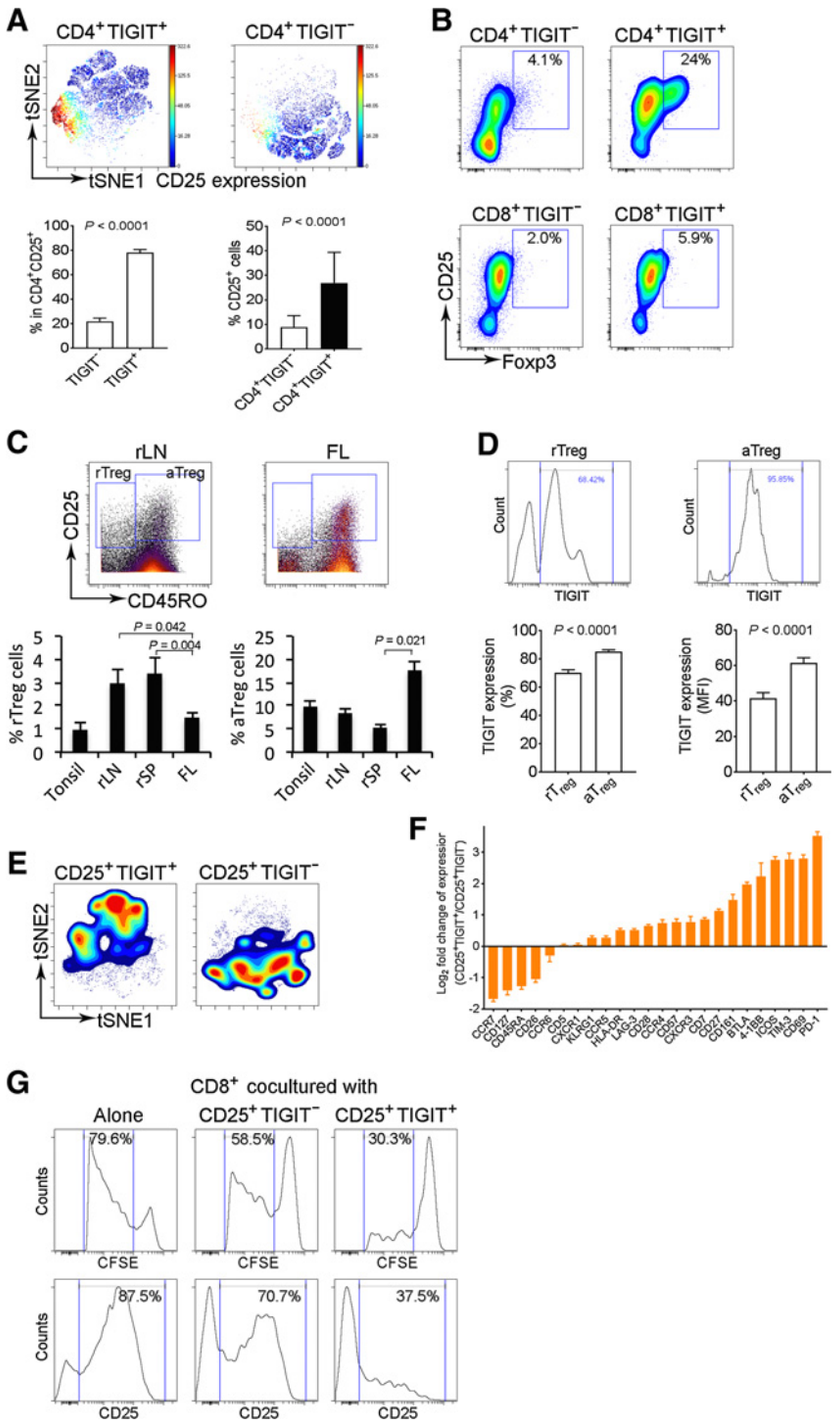

Figure 2.

TIGIT is preferentially expressed on activated T_{reg} cells with enhanced suppressive properties. **A,** The viSNE plots showing CD25 expression by TIGIT$^+$ or TIGIT$^-$ CD4$^+$ cells. Graphs below showing percentage of TIGIT$^+$ or TIGIT$^-$ cells in CD4$^+$CD25$^+$ population (left) or percentage of CD25$^+$ cells in TIGIT$^+$ or TIGIT$^-$ CD4$^+$ cells ($n = 82$). **B,** Dot plots showing expression of CD25 and Foxp3 by TIGIT$^-$ or TIGIT$^+$ CD4$^+$ or CD8$^+$ cells. T cells from healthy donor were cultured in an anti-CD3 Ab-coated plate in the presence of anti-CD28 Ab for 5 days and expression of CD25 and Foxp3 on gated TIGIT$^-$ or TIGIT$^+$ CD4$^+$ or CD8$^+$ cells was measured by flow cytometry. **C,** Dot plots showing coexpression of CD45RA and CD25 to define rT_{reg} (CD45RA$^+$CD25$^+$) or aT_{reg} (CD45RA$^-$CD25$^+$) from a representative rLN or follicular lymphoma biopsy specimen. Graph below showing percentage of rT_{reg} and aT_{reg} in CD4$^+$ population in tonsil, rLN, rSP, or follicular lymphoma, $n = 82$. **D,** Histograms showing TIGIT expression by rT_{reg} or aT_{reg} cells and graphs below showing percentage of TIGIT$^+$ cells (left) or TIGIT expression level (MFI, right) in rT_{reg} or aT_{reg} cells. **E,** The viSNE plots (contour) of TIGIT$^+$ or TIGIT$^-$ CD25$^+$ cells from follicular lymphoma. The tSNE analysis was performed on a concatenated file ($n = 82$). **F,** Graph showing fold change (log_2) of surface marker expression in TIGIT$^+$ versus TIGIT$^-$ CD25$^+$ cells. **G,** Histograms showing CFSE staining and expression of CD25 by CD8$^+$ cells cocultured alone or with TIGIT$^+$ or TIGIT$^-$ CD25$^+$ cells.

TIGIT$^-$ and TIGIT$^+$ cells. This result indicated that T_H1 cells accounted for the majority of non-T_{reg}/T_{FH} TIGIT$^+$CD4$^+$ in follicular lymphoma.

As a mixed population, we then characterized the phenotype of the non-T_{reg}/T_{FH} TIGIT$^+$CD4$^+$ population using a tSNE analysis. Nine distinct subsets (S1–S9) were identified and the frequency ranged from 2.4% to 14.5% ($n = 82$; **Fig. 3F**). Although each subset possessed a unique phenotype, some subsets were largely distinct from other subsets and some only modestly different from others (**Fig. 3G**). All subsets lacked CD45RA expression, identifying a memory phenotype for this population. In addition, all subsets had variable expression of CD5 and CD28 as well as some expression of HLA-DR. One (S1) and two (S7 and S8) subsets lacked expression of CD7 and CD27, respectively. S3 and S4 expressed CCR7, suggesting a central memory (T_{CM}) phenotype. PD-1 was expressed on most subsets except two (S3 and S4), suggesting that the majority of the non-T_{reg}/T_{FH} TIGIT$^+$CD4$^+$

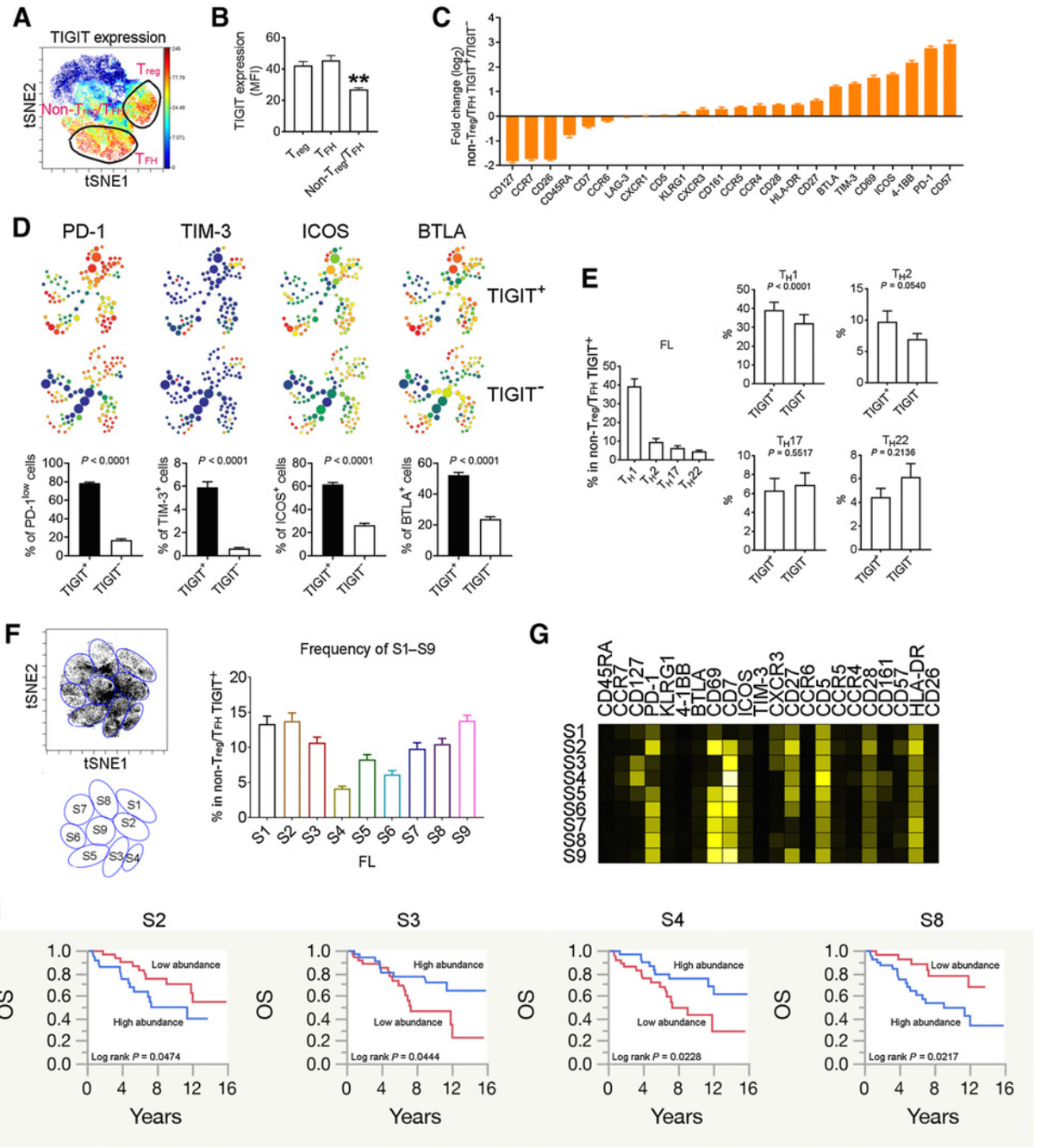

Figure 3.

TIGIT expression defines intratumoral non-T_{reg}/T_{FH} $CD4^+$ cells as exhausted cells. **A,** The viSNE plots showing expression of TIGIT on T_{reg}, T_{FH}, and non-T_{reg}/T_{FH} cells. **B,** Graph showing TIGIT expression level by MFI on T_{reg}, T_{FH}, and non-T_{reg}/T_{FH} cells. **, $P < 0.01$ when comparing with both T_{reg} and T_{FH}. **C,** Graph showing fold change (log_2) of surface marker expression in $TIGIT^+$ versus $TIGIT^-$ non-T_{reg}/T_{FH} cells. **D,** SPADE maps showing expression of PD-1, TIM-3, ICOS, or BTLA on $TIGIT^+$ or $TIGIT^-$ non-T_{reg}/T_{FH} cells. The dots in blue or in red indicate low or high expression, respectively. The dots with big size contain more cell events. Graphs (below) showing percentage of PD-1^+, TIM-3^+, $ICOS^+$, or $BTLA^+$ cells in $TIGIT^+$ or $TIGIT^-$ non-T_{reg}/T_{FH} cells. **E,** Graph (left) showing percentage of T_H1, T_H2, T_H17, or T_H22 in $CD4^+$ non-T_{reg}/T_{FH} cells. See Supplementary Fig. 2 for identification of these T_H subsets. Graphs (right) showing percentage of T_H1, T_H2, T_H17, or T_H22 in $TIGIT^+$ or $TIGIT^-$ non-T_{reg}/T_{FH} cells, $n = 82$. **F,** The viSNE plot showing cell subsets from a representative patient sample. Subsets were identified on the basis of viSNE plots in which cells with similar phenotype were clustered together. Graph (right) showing percentage of each subset in $TIGIT^+$ non-T_{reg}/T_{FH} cells, $n = 82$. **G,** Heatmap showing median intensity of each marker for subsets identified above. **H,** Kaplan–Meier curves of overall survival of subsets of S2, S3, S4, and S8 in patients with follicular lymphoma ($n = 82$).

cells were exhausted cells. We then tested whether any of these non-T_{reg}/T_{FH} subsets were associated with patient outcome and found that S2 and S8 were associated with an inferior overall survival and S3 and S4, in contrast, correlated with a favorable overall survival using the median number of cells as a cut point (**Fig. 3H**). This result correlated with PD-1 expression (exhaustion) on cells from S2 and S8, while cells from S3 and S4 lacked PD-1 expression (**Fig. 3G**). Consistent with patient survival results, we observed that the number of cells from S4 was significantly higher in patients who achieved EFS24 than patients who failed EFS24 (Supplementary Fig. S3A). Cox regression analysis showed a higher risk ratio for S2 and S8 and a low risk ratio for S3 and S4, meaning a worse and better overall survival for S2/S8 and S3/S4, respectively (Supplementary Table 3). Together, these findings suggested a correlation between T-cell exhaustion and patient survival.

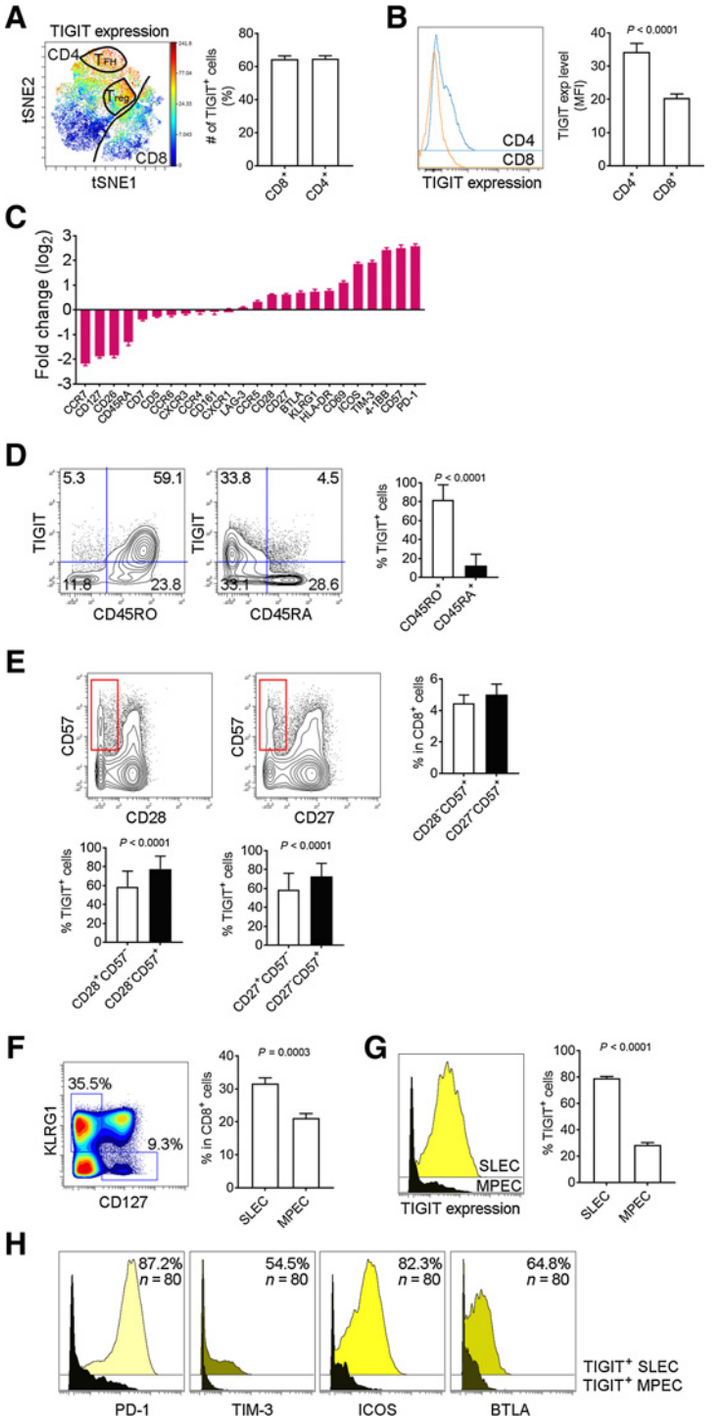

Figure 4.

TIGIT is involved in CD8$^+$ T-cell differentiation and is preferentially expressed on late-stage memory cells. **A,** The viSNE plot showing TIGIT expression on CD4$^+$ and CD8$^+$ cells. Graph (right) showing percentage of TIGIT$^+$ cells on CD4$^+$ or CD8$^+$ cells in follicular lymphoma, $n = 82$. **B,** Histogram from a representative follicular lymphoma sample (left) and graph (right) showing TIGIT expression level on CD4$^+$ or CD8$^+$ cells, $n = 82$. **C,** Graph showing fold change (log_2) of surface marker expression in TIGIT$^+$ versus TIGIT$^-$ CD8$^+$ cells. **D,** Dot plots showing coexpression of TIGIT and CD45RO or CD45RA in CD8$^+$ T cells. Graph (right) summarizes percentage of TIGIT$^+$ cells in CD8$^+$CD45RO$^+$ or CD8$^+$CD45RA$^+$ T cells in follicular lymphoma. **E,** Dot plots showing coexpression of CD57 and CD28 or CD27 in CD8$^+$ T cells. Graph (right) summarizes percentage of CD28$^+$CD57$^+$ and CD27$^+$CD57$^+$ in CD8$^+$ T cells in follicular lymphoma. Graphs (below) summarizes TIGIT$^+$ cells in CD28$^+$CD57$^+$ or CD28$^-$CD57$^+$ as well as CD27$^+$CD57$^+$ or CD27$^-$CD57$^+$ T cells in follicular lymphoma. **F,** Dot plots showing coexpression of CD127 and KLRG1 to define SLEC (CD127$^-$KLRG1$^+$) and MPEC (CD127$^+$KLRG1$^-$). Graph (right) summarizes percentage of SLEC and MPEC in CD8$^+$ T cells from follicular lymphoma, $n = 82$. **G,** Histogram showing TIGIT expression by SLEC and MPEC. Graph (right) summarizes percentage of TIGIT$^+$ cells in SLEC and MPEC subset from follicular lymphoma, $n = 82$. **H,** Histogram showing PD-1, TIM-3, ICOS, or BTLA on TIGIT$^+$ SLEC or MPEC subset.

TIGIT is preferentially expressed on late-stage memory CD8$^+$ T cells

In addition to its expression on CD4$^+$ T cells, TIGIT is also expressed on intratumoral CD8$^+$ T cells and approximately 61.9% of CD8$^+$ T cells expressed TIGIT (**Fig. 4A**). Expression levels of TIGIT on CD8$^+$ T cells were substantially lower when compared with CD4$^+$ T cells, although the number of TIGIT-expressing CD4$^+$ and CD8$^+$ T cells was quite comparable (**Fig. 4B**). The higher expression level of TIGIT on CD4$^+$ T cells is attributed to abundant expression on the T_{reg} and T_{FH} subsets. These results suggest that TIGIT is highly expressed on specialized subsets (T_{reg} and T_{FH}) with lower level expression on exhausted T cells (CD4$^+$ and CD8$^+$). Similar to TIGIT$^+$CD4$^+$ T cells, TIGIT$^+$CD8$^+$ T cells displayed a memory phenotype as the number of cells expressing CD45RA, CCR7, and CD127 were lower in TIGIT$^+$ cells than TIGIT$^-$ cells. In addition, CD8$^+$TIGIT$^+$ T cells displayed an immune exhaustion phenotype, as expression of inhibitory receptors PD-1, TIM-3, LAG-3, BTLA, and ICOS were increased when compared with CD8$^+$TIGIT$^-$ cells (**Fig. 4C**).

Next, we assessed whether TIGIT is involved in intratumoral CD8$^+$ T-cell differentiation. The finding that TIGIT was predominantly expressed on memory (CD45RO$^+$) cells and modestly on naïve (CD45RA$^+$) cells indicated that TIGIT is involved in intratumoral CD8$^+$ T-cell differentiation (**Fig. 4D**). Conversion from CD28$^+$CD57$^-$ or CD27$^+$CD57$^-$ to CD28$^-$CD57$^+$ or CD27$^-$CD57$^+$ represents a path of CD8$^+$ T-cell differentiation under conditions of persistent immune stimulation. As shown in **Fig. 4E**, approximately 4.5% and 5.1% CD8$^+$ T cells had differentiated into CD28$^-$CD57$^+$ or CD27$^-$CD57$^+$ in follicular lymphoma, respectively. Compared with CD28$^+$CD57$^-$ or CD27$^+$CD57$^-$ CD8$^+$ T cells, CD28$^-$CD57$^+$ or CD27$^-$CD57$^+$ CD8$^+$ T cells showed a significantly increased TIGIT expression, suggesting that TIGIT is preferentially expressed by late-stage memory cells (**Fig. 4E**).

CD8$^+$ effector cells consist of subsets of short-lived effector cells (SLEC) and memory–precursor effector cells (MPEC) defined by expression of CD127 and KLRG1. In follicular lymphoma, SLECs (KLRG1$^+$CD127$^-$) and MPECs (CD127$^+$KLRG1$^-$) accounted for approximately 31.5% (range, 6.5%–82.3%, $n = 80$) and 20.9% (range, 0.8%–49.1%, $n = 80$) of intratumoral CD8$^+$ T cells, respectively (**Fig. 4F**). Although its expression was not completely absent on MPECs, TIGIT was abundantly expressed on SLECs (**Fig. 4G**). In follicular lymphoma, TIGIT was expressed on approximately 79.3% (range, 30.7%–97.5%, $n = 80$) and 28.8% (range, 4.9%–67.5%, $n = 80$) of intratumoral MPECs and SLECs, respectively (**Fig. 4G**). These TIGIT$^+$ SLECs also exhibited an exhaustion phenotype. As shown in **Fig. 4H**, TIGIT$^+$SLECs expressed inhibitory receptors including PD-1, TIM-3, ICOS, and BTLA and the percentage of TIGIT$^+$ cells expressing PD-1, TIM-3, ICOS, or BTLA cells was 87.2%, 54.5%, 82.3%, and 64.8%, respectively. Taken together, these results suggest that TIGIT is involved in CD8$^+$ T-cell differentiation and TIGIT$^+$CD8$^+$ T cells exhibit a phenotype of exhaustion.

TIGIT expression correlates with an unfavorable survival in patients with follicular lymphoma

Given a broad expression of TIGIT and its role in defining T subsets that mediate distinct immune responses, we explored the clinical relevance TIGIT expression had in follicular lymphoma. To test this, we measured the number of TIGIT$^+$ T cells in biopsy specimens, as well as clinical parameters, in a cohort of 82 untreated follicular lymphoma patients that had a follow-up for approximately 20 years. We observed that intratumoral CD3$^+$TIGIT$^+$ cells were differentially represented in patient groups defined by clinical parameters. As shown in **Fig. 5A**, the frequency of CD3$^+$TIGIT$^+$ cells was significantly higher in patients older than 60 years and patients who had an elevated lactate dehydrogenase at diagnosis. In contrast, patients with hemoglobin (HGB) < 12 g/dL at diagnosis showed decreased numbers of CD3$^+$TIGIT$^+$ cells when compared with patients with HGB > 12 g/dL at diagnosis. Interestingly, patients who had reduced numbers of CD3$^+$TIGIT$^+$ cells were more likely to respond to therapy, as the numbers of CD3$^+$TIGIT$^+$ cells were significantly lower in patients who had complete (CR) or partial remission (PR) than patients who had no response or progression (**Fig. 5A**). We did not see a difference of frequency of CD3$^+$TIGIT$^+$ cells correlating with other clinical parameters such as histology (follicular grade 1/2 vs. 3a/b), stage (I/II vs. III/IV), B symptoms (yes vs. no), number of lymph node sites (1–3 vs. ≥4), follicular lymphoma IPI scores (1–2 vs. 3–5), absolute lymphocyte count (greater than 0.89×10^9/l vs. less than 0.89×10^9/l) and EFS24 (achieved vs. failed).

We then determined whether the numbers of intratumoral TIGIT$^+$ T cells correlated with EFS or OS in patients with follicular lymphoma. We extracted TIGIT$^+$ T-cell numbers as the percentages among CD3$^+$, CD4$^+$, or CD8$^+$ T cells (CD3$^+$TIGIT$^+$, CD4$^+$TIGIT$^+$, or CD8$^+$TIGIT$^+$) from the cohort of 82 patients with follicular lymphoma. Using the Kaplan–Meier method and the median number as a cut-off point, we found that an increased number of CD3$^+$TIGIT$^+$ T cells was significantly associated with an inferior EFS ($P = 0.0276$) as well as a poorer OS ($P = 0.0151$; **Fig. 5B**). Consistent with this finding, RNA sequencing analysis revealed that TIGIT RNA expression level correlated with a worse outcome in patients with follicular lymphoma, although a statistical significance was not achieved ($P = 0.0872$ for OS and $P = 0.0703$ for EFS; Supplementary Fig. S4A). Similar results were seen in subsets of CD4$^+$TIGIT$^+$ or CD8$^+$TIGIT$^+$ T cells (**Fig. 5B**). This correlation was independent of other immune inhibitory receptors, as TIGIT was the only receptor that significantly correlated with patient survival when analyzed using a multivariate method (Supplementary Table 3). The Cox regression analysis showed a higher risk ratio for CD3$^+$TIGIT$^+$, CD4$^+$TIGIT$^+$, or CD8$^+$TIGIT$^+$ T subsets, consistent with the above survival findings (Supplementary Table S3). To exclude impact of therapy on TIGIT-associated patient survival, we selected a cohort of patients who were observed and received no treatment and performed the Kaplan–Meier analysis. Similar results were observed, in that increased number of TIGIT$^+$ T cells correlated with an inferior overall and event-free survival in follicular lymphoma (Supplementary Fig. S4B).

Immune signatures from CD8$^+$TIGIT$^+$ contribute to TIGIT-associated survival in follicular lymphoma

Given the reduced function and inferior survival association of TIGIT$^+$ T cells in follicular lymphoma, we questioned which phenotype (immune signature) could contribute to TIGIT-associated clinical outcomes. Clinical endpoint EFS24 and survival (alive vs. dead) was used to address this question. Using CITRUS analysis, we identified 6 clusters (red dots) that differed between patients who failed or achieved EFS24 (**Fig. 6A**, i). Two clusters (261915 and 281914) came from the CD8$^+$TIGIT$^+$ population and the other four from the CD4$^+$TIGIT$^+$ population with parent cluster 261931. As a result, these clusters exhibited a similar phenotype. Two CD8$^+$ clusters (261915 and 281914) showed a typical exhausted phenotype of PD-1^{low}TIM-3$^+$ expression (**Fig. 6A**, ii). The abundance of these clusters was higher in the patients who failed EFS24 than those who achieved EFS24 (**Fig. 6A**, iii). Next, using the same analysis, we compared two groups of patients who remain alive and patients who died and identified 4 clusters (red dots) that differed between these patient groups (**Fig. 6B**, i). All these 4

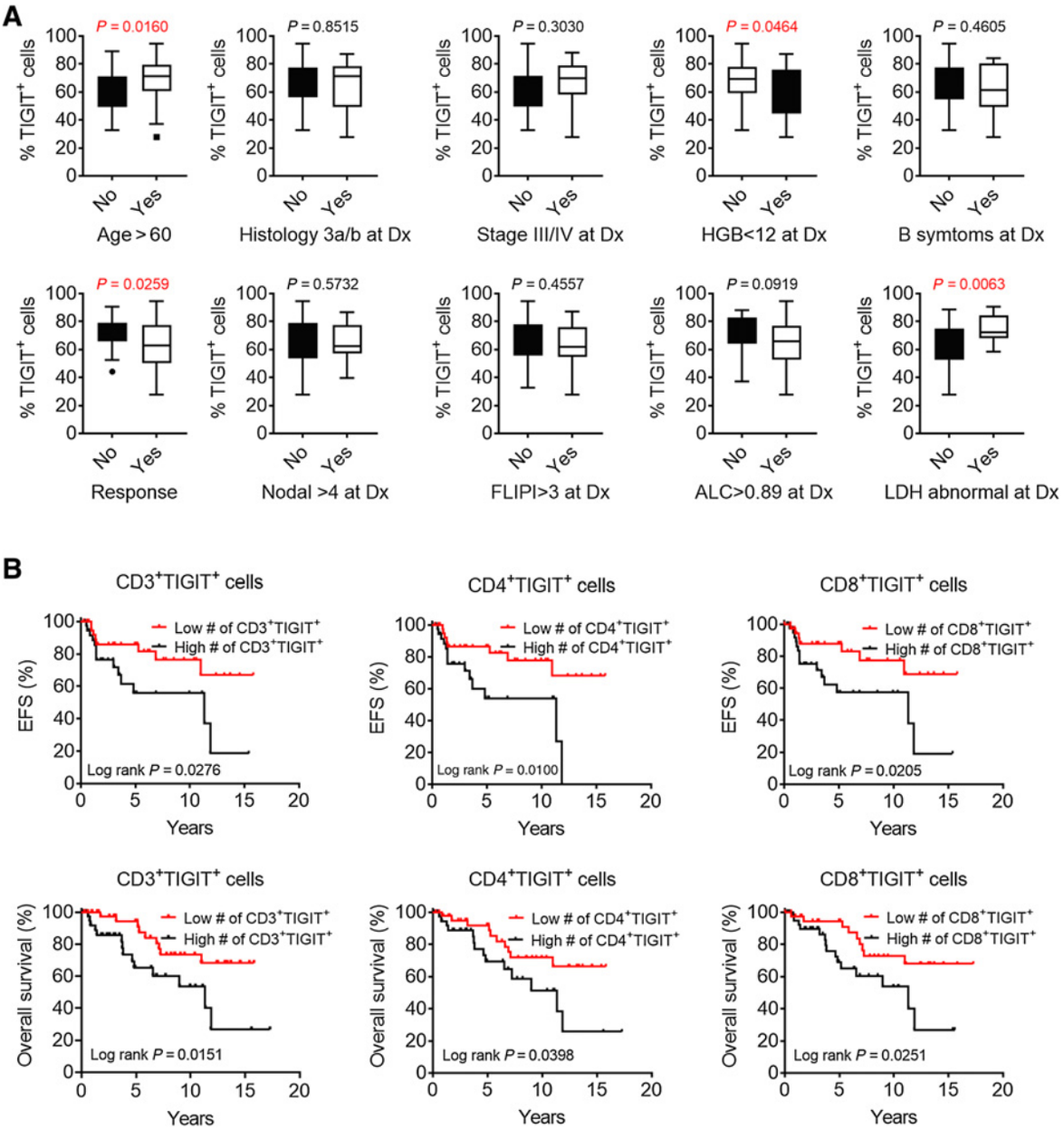

Figure 5.

TIGIT expression correlates an unfavorable survival in patients with follicular lymphoma. **A,** Graphs showing percentage of TIGIT$^+$ T cells in two patient groups. Patients with follicular lymphoma were grouped using age (older than 60 vs. not), histology (grade 1/2 vs. 3a/b), stage (I/II vs. III/IV), hemoglobin (HGB) level (<12 g/dL vs. ≥12 g/dL), B symptoms (no vs. yes), treatment response (no vs. yes), nodal number (more than 4 vs. not), FLIPI score (greater than 3 vs. not), absolute lymphocyte counts (ALC, $<0.89 \times 10^9$/l vs. $\geq 0.89 \times 10^9$/l), and lactate dehydrogenase (LDH) level (abnormal vs. not). **B,** Kaplan–Meier curves for OS or EFS of patients with follicular lymphoma ($n = 82$) by the number of TIGIT$^+$ CD3$^+$, CD4$^+$, and CD8$^+$ cells with a cutoff of 68.2%, 66.8%, and 68.5%, respectively.

clusters (79592, 79580, 79605, and 79609) came from CD8$^+$TIGIT$^+$ population. Cluster 79609 was a parent cluster that divided cells to form clusters 79605, 79580, and 79592. Therefore, these 4 clusters showed a similar phenotype and all had reduced levels of ICOS, PD-1, CD26, BTLA, CD161, and CD57, and increased levels of CXCR3, CCR7, CD127, and KLRG1 (**Fig. 6B**, ii), suggesting a less exhausted phenotype. The abundance of these clusters was higher in the patients who were alive than those who died (**Fig. 6B**, iii). These results suggest that TIGIT$^+$CD8$^+$ T cells may play a major role in TIGIT-associated clinical outcome in follicular lymphoma. Given the unique phenotype of these clusters, we wondered whether any of these clusters had prognostic impact in follicular lymphoma. By extracting the abundance events of these 4 clusters from each patient of this cohort, we analyzed survival curve using the Kaplan–Meier method. We observed that increased abundance of clusters 79605, 79580, and 79592 was associated with a better overall survival using the median number as

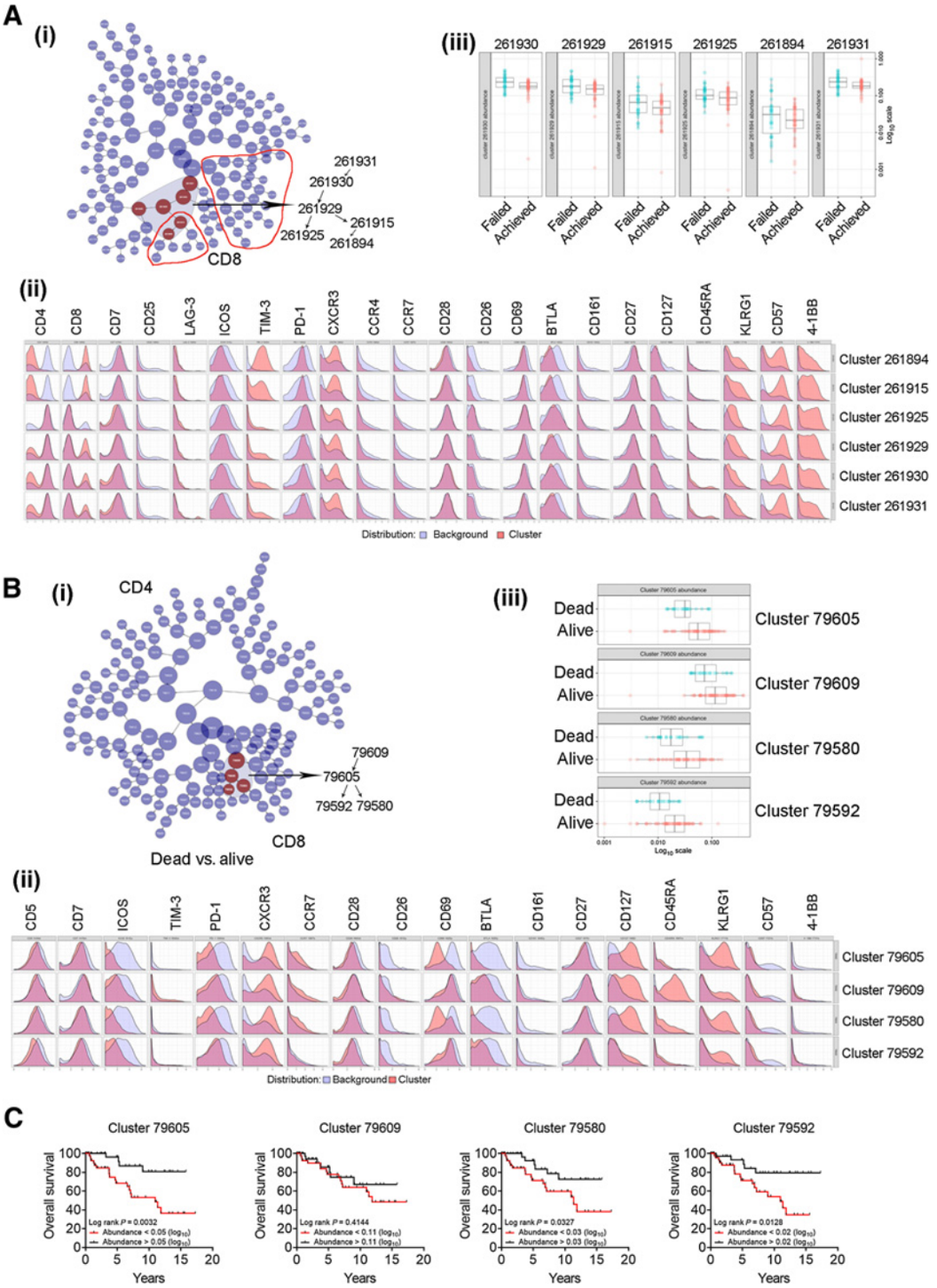

Figure 6.

Immune signatures from CD8$^+$TIGIT$^+$ contribute to TIGIT-associated survival in follicular lymphoma. **A** (i) or **B** (i), CITRUS plot showing clustering results from patients with follicular lymphoma divided by 2 groups (EFS24 failed vs. achieved) or (patients alive vs. dead). Circles in red represent clusters that differed between groups. Number in circles indicates a cluster ID. **A** (ii) or **B** (ii), Histogram plots showing expression of selected markers by cells from all clusters overlaid on background staining. Expression level of each selected marker was expressed by cluster (red) over background (light blue). **A** (iii) or **B** (iii), Graph showing quantitative results of abundance from all clusters. **C,** Kaplan–Meier curves for OS of patients with follicular lymphoma ($n = 82$) by the abundance of 4 clusters.

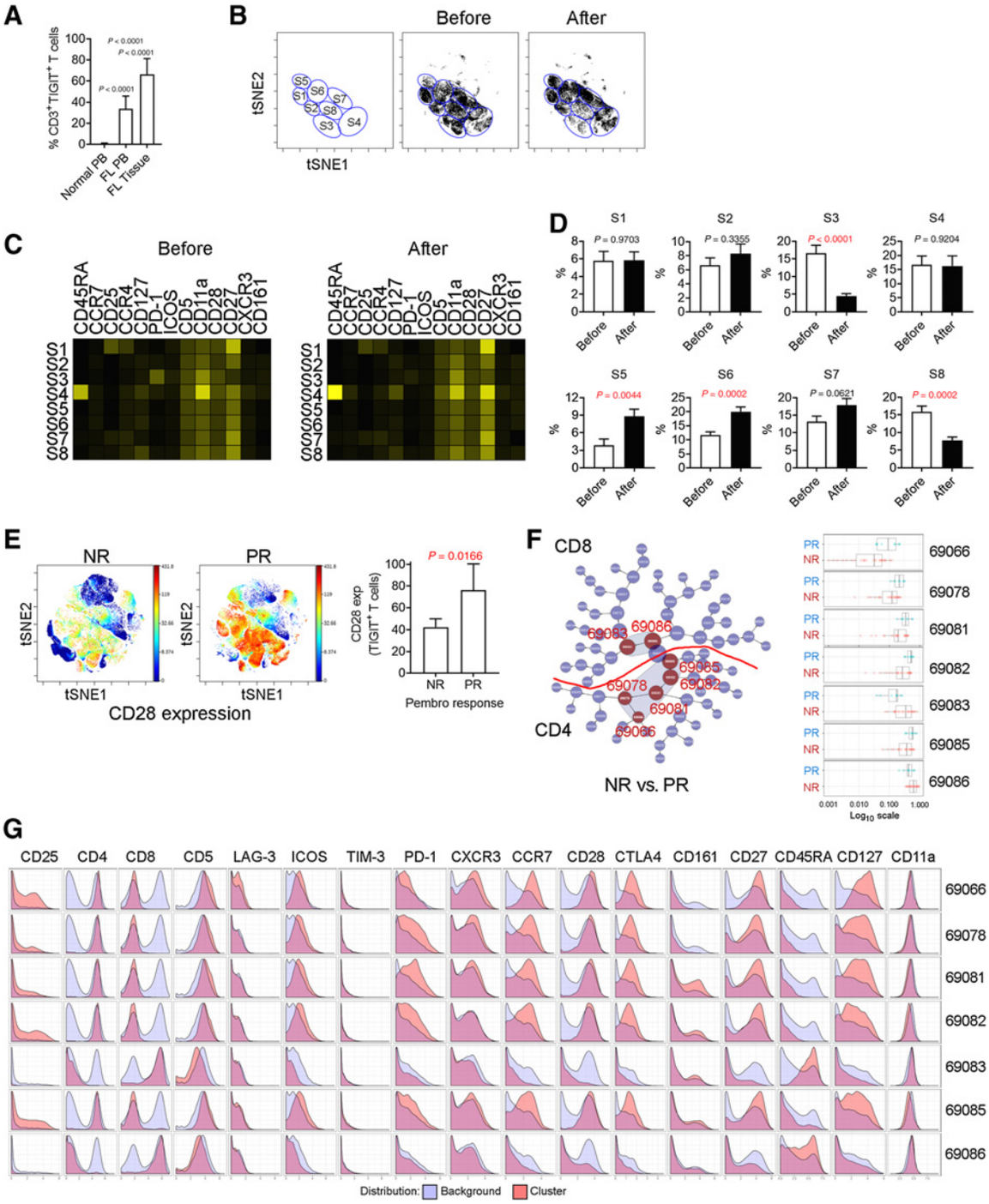

Figure 7.

PD-1 immunotherapy targets exhausted TIGIT subsets in follicular lymphoma. **A,** Graph showing percentage of $CD3^{+}TIGIT^{+}$ T cells in normal PB, follicular lymphoma PB, and follicular lymphoma tissue. **B,** The viSNE plots showing cell subsets from a representative patient sample before and after pembrolizumab treatment. Subsets were identified on the basis of viSNE plots in which cells with similar phenotype were clustered together. **C,** Heatmap showing median intensity of each marker for subsets identified above in a representative patient sample before and after pembrolizumab treatment. **D,** Graphs summarize the percentage of each subset in patients before and after treatment ($n = 21$). **E,** The viSNE plots showing CD28 expression in representative patients with partial response or no response. Graph (right) summarizes the percentage of CD28 expression level in $TIGIT^{+}$ T cells in patients with partial response or no response. **F,** CITRUS plot showing clustering results from patients with follicular lymphoma divided by 2 groups (NR vs. PR). Circles in red represent clusters that differed between groups. Number in circles indicates a cluster ID. Graph on the right showing quantitative results of abundance from 7 clusters. **G,** Histogram plots showing expression of selected markers by cells from 7 clusters overlapped to background. Expression level of each selected marker was expressed by cluster (red) over background (light blue).

the cut-off point (**Fig. 6C**), which is consistent with the finding that these 3 clusters shared similar phenotype. Supporting this finding, Cox regression analysis showed a lower risk ratio for all 4 clusters, and a better OS (Supplementary Table S3). Given these clusters had less exhausted phenotypes, these results suggest that T-cell exhaustion, especially $CD8^+$ exhaustion, contributed to TIGIT-associated survival in follicular lymphoma.

PD-1 immunotherapy targets exhausted TIGIT subsets in follicular lymphoma

Immunotherapy, especially anti–PD-1 therapy, has improved the outcome of patients with cancer by promoting an antitumor T-cell response. Given that TIGIT is coexpressed with PD-1 on exhausted T cells in follicular lymphoma, we next determined whether PD-1–mediated immunotherapy had an effect on TIGIT subsets, particularly those with an exhausted phenotype. Using specimens from a clinical trial of pembrolizumab, an FDA-approved anti–PD-1 Ab, in 21 patients with relapsed or refractory follicular lymphoma, PB from these patients collected before and after pembrolizumab therapy was analyzed using CyTOF. As shown in **Fig. 7A**, TIGIT was more abundantly expressed on PB T cells from follicular lymphoma than healthy donors, although at lower levels than what was seen on intratumoral T cells. $TIGIT^+$ T cells accounted for approximately 36.2% of the total T cells from PB compared with 62.4% in biopsy specimens from follicular lymphoma. Anti–PD-1 therapy did not alter TIGIT expression as no significant difference of the numbers of $TIGIT^+$ T cells ($CD3^+$, $CD4^+$, or $CD8^+$) was seen between patients before or after the treatment (Supplementary Fig. S5A). However, we found that anti–PD-1 therapy had an effect on phenotypes of $CD4^+TIGIT^+$ T cells by altering the numbers of $TIGIT^+$ subsets. $TIGIT^+$ subsets were defined by tSNE analysis and 8 subsets (S1–S8) of $CD4^+TIGIT^+$ T cells were determined on the basis of phenotypic difference (**Fig. 7B**). S1 and S7 were two subsets having CD25 expression, therefore, classified into T_{reg} cell subsets. S4 displayed CD45RA expression and constituted both naïve and terminally differentiated cells based on CCR7 expression status (**Fig. 7C**). It appeared that these 3 subsets did not respond to anti–PD-1 therapy as the percentage of cell numbers showed no significant difference before and after pembrolizumab. Among other 5 subsets of memory cells, S3 and S8 exhibited phenotypical features of exhaustion when compared to S5 and S6 as S3 and S8 expressed increased inhibitory markers such PD-1, TIM-3, ICOS, and LAG-3 (Supplementary Fig. S5B). Although S3 and S8 were suppressed by anti–PD-1 therapy, S5 and S6 that displayed a less exhausted phenotype were expanded after pembrolizumab treatment (**Fig. 7D**). These results suggest that anti–PD-1 therapy targeted $TIGIT^+$ exhausted T-cell populations and promoted expansion of $TIGIT^+$ effector cells.

In the current cohort, 4 patients achieved a PR after pembrolizumab. By comparing these 4 patients to nonresponders (NR), we found that patients who had a higher level of CD28 expression on $TIGIT^+$ T cells were more likely to achieve a response to pembrolizumab than patients who had low CD28 expression on $TIGIT^+$ T cells (**Fig. 7E**). The number of $TIGIT^+CD28^-$ T cells was significantly lower in responders than nonresponders. Of note, there was a weak positive association between TIGIT and CD28 expression, in that higher TIGIT expression correlated with higher CD28 expression on $PD\text{-}1^+$ cells (data not shown).

We next wondered which clusters contribute to the clinical efficacy (NR vs. PR) of pembrolizumab. By CITRUS analysis, we identified 7 clusters that differed between patients with NR and PR. Five clusters were from $CD4^+TIGIT^+$ T cells and two from $CD8^+TIGIT^+$ T cells. Although the abundance of all clusters from $CD4^+TIGIT^+$ T cells increased, the abundance of clusters from $CD8^+TIGIT^+$ T cells decreased in patients with a PR after anti–PD-1 therapy (**Fig. 7F**). Interestingly, all clusters from $CD4^+TIGIT^+$ T cells showed increased CD28 and CD27 expression while clusters from $CD8^+TIGIT^+$ T cells (69083 and 69086) displayed decreased CD28 and CD27 expression (**Fig. 7G**). By comparing CD28 expression on $CD4^+TIGIT^+$ and $CD8^+TIGIT^+$ T cells, we observed that CD28 loss was dramatic as approximately 65.1% of $CD8^+TIGIT^+$ T cells lost CD28 expression when compared with 11.6% of $CD4^+TIGIT^+$ T cells (Supplementary Fig. S5C).

Discussion

Intratumoral T cells are the major component of antitumor immunity and impact patient outcome in follicular lymphoma (21–23), although intratumoral macrophages also play a crucial role in mediating the immune response and may negatively affect clinical outcomes (24–30). From preclinical and clinical observations, molecules from the immune checkpoint family play a crucial role in regulating antitumor immunity in lymphomas (31–33). TIGIT, a member of this family, is no exception (14, 15). TIGIT was initially identified to be expressed on regulatory, memory, and activated T cells (1) and subsequently shown to be expressed on other T cells, including T_{reg} and T_{FH} cells. Intratumoral T cells exhibit robust TIGIT expression as nearly all major subsets of $TIGIT^+$ T cells are present in the tumor microenvironment. We observed multiple $TIGIT^+$ subsets including effector memory cells, T_{reg}, T_{FH}, and exhausted cells, and these subsets exist in substantial numbers in follicular lymphoma. Broad expression of TIGIT on intratumoral T cells may magnify its impact on anti-immunity, thereby affecting patient outcomes as shown in the current study.

It has been shown that TIGIT is expressed on T_{reg} cells (34, 35) and we found that T_{reg} cells were the major T-cell subset to express TIGIT in follicular lymphoma. The finding that Foxp3 and TIGIT were co-induced on activated $CD4^+$ T cells *in vitro* indicated that TIGIT and T_{reg} cells ($Foxp3^+$ cells) are intrinsically correlated. TIGIT expression was strong and abundant on most intratumoral T_{reg} cells in follicular lymphoma and lack of TIGIT expression resulted in a distinct phenotype of T_{reg} cells. For example, a number of functional T-cell markers including CD7, CD27, and CD28, as well as CD69 and 4-1BB, are highly expressed on $TIGIT^+$ T_{reg} cells when compared with $TIGIT^-$ T_{reg} cells, which is consistent with a previous report (36). These findings may make TIGIT highly relevant to T_{reg} cell function and we found that TIGIT is preferentially expressed on a more functional T_{reg} cell type (highly functional aT_{reg} compared with a less functional rT_{reg}). Supporting this finding, $TIGIT^+$ T_{reg} cells showed increased suppression of $CD8^+$ T cells when compared to $TIGIT^-$ T_{reg} cells. The finding that $TIGIT^+$ T_{reg} cells express more functional receptors than $TIGIT^-$ T_{reg} cells may contribute to increased function of $TIGIT^+$ T_{reg} cells over $TIGIT^-$ T_{reg} cells. A previous study revealed that TIGIT signaling restores suppressor function of T_H1 T_{reg} cells through repression of Akt, reiterating a role of TIGIT in T_{reg} function (37).

In follicular lymphoma, TIGIT is expressed on a substantial number of intratumoral $CD4^+$ T cells that are not T_{reg} or T_{FH} (non-T_{reg}/T_{FH}) cells. These non-T_{reg}/T_{FH} $TIGIT^+$ cells expressed increased levels of inhibitory receptors such as PD-1, TIM-3, ICOS, and BTLA when compared with $TIGIT^-$ cells, indicating an immunologically exhausted population, which is consistent with data, suggesting that TIGIT functions as an immune-checking molecule and contributes to

T-cell exhaustion (38–40). The non-T_{reg}/T_{FH} $TIGIT^+$ cells consisted of T_H subsets with predominance of T_H1 cells. Subsets identified by viSNE analysis demonstrated the prevalence of T_H1 cells and fewer T_H2, T_H17, and T_H22 cells in non-T_{reg}/T_{FH} $TIGIT^+$ fraction, consistent with our previous studies (32, 41).

TIGIT is also expressed on intratumoral $CD8^+$ T cells with expression levels similar to non-T_{reg}/T_{FH} $CD4^+$ cells but lower than T_{reg} and T_{FH} cells. These results suggest that high expression of TIGIT defines specialized subsets (T_{reg} and T_{FH}) and dim expression defines exhausted T cells ($CD4^+$ and $CD8^+$), a finding similar to PD-1 expression in which high expression of PD-1 defines specialized subsets (T_{FH}) and dim expression defines exhausted T cells ($CD4^+$ and $CD8^+$; ref. 31). $TIGIT^+CD8^+$ T cells exhibited a distinct phenotypical profile when compared with $TIGIT^-CD8^+$ T cells and expressed multiple inhibitory receptors including PD-1, TIM-3, ICOS, and BTLA, suggesting an exhaustion phenotype similar to that seen in other types of cancers (9, 14, 40). An interesting finding is that TIGIT is involved in $CD8^+$ T cell differentiation. It has been shown that loss of CD28 or CD27 expression represents T cells in the late stage of differentiation and gain of CD57 expression on $CD28^-$ or $CD27^-$ $CD8^+$ T cells identifies them as terminally differentiated cells (42–44). The path from $CD28^+CD57^-$ or $CD27^+CD57^-$ to $CD28^-CD57^+$ or $CD27^-CD57^+$ reflects $CD8^+$ T-cell differentiation under conditions of persistent immune stimulation. We observed that TIGIT is highly expressed by $CD28^-CD57^+$ or $CD27^-CD57^+$ $CD8^+$ T cells, rather than $CD28^+CD57^-$ or $CD27^+CD57^-$ $CD8^+$ T cells. Consistent with this finding, we found that TIGIT is preferentially expressed on short-lived effector memory $CD8^+$ cells. Taken together, these results indicate that TIGIT is highly expressed on late-stage $CD8^+$ T cells and may be involved in $CD8^+$ T-cell differentiation.

Despite extensive investigations (12, 38, 40, 45), studies regarding the role of TIGIT in cancer patient survival are limited. In patients with AML, high TIGIT expression correlates with primary refractory disease and leukemia relapse post-alloSCT (9). In hepatitis B virus–associated hepatocellular carcinoma (HBV-HCC), $PD\text{-}1^+TIGIT^+CD8^+$ T-cell populations were negatively correlated with overall survival and progression-free survival rates (46). Consistent with these findings, we observed that increased numbers of $TIGIT^+$ T cells are associated with an inferior survival in follicular lymphoma. We have previously shown that intratumoral $PD\text{-}1^{high}$ or $PD\text{-}1^{low}$ CD4/CD8 T cells are differentially prognostic (31). In the current study, we observed a similar finding that $TIGIT^{high}$ or $TIGIT^{low}$ CD4/CD8 T cells are differentially prognostic, which may be attributed to coexpression of TIGIT with PD-1. Clustering analysis showed that $CD8^+$ T cells with an exhaustion phenotype mainly contribute to TIGIT-associated inferior survival, consistent with other studies (9, 46).

Given coexpression of TIGIT and PD-1 on exhausted T cells, we determined whether $TIGIT^+$ T-cell subsets responded to anti–PD-1 Ab therapy in patients with relapsed and/or refectory follicular lymphoma. We observed that while $TIGIT^+$ T cells as a whole did not respond, subsets of $TIGIT^+$ T cells responded to pembrolizumab treatment differentially. $TIGIT^+$ subsets with an exhaustion phenotype are downregulated and the subsets with effector phenotypes are upregulated by pembrolizumab therapy, respectively. This finding may suggest a potential mechanism for anti–PD-1 therapy in that pembrolizumab inhibits exhausted T cells and promotes the expansion of functionally active effector cells. Supporting this, patients with follicular lymphoma with high expression of CD28 on $TIGIT^+$ T cells responded to pembrolizumab compared with patients showing no response. This finding is also consistent with previous studies identifying CD28 as the primary target for PD-1–targeted therapy (47, 48). In the current study, we found that the function of $TIGIT^+$ T cells is diminished, but that blocking TIGIT signaling restores T-cell function (10, 49). On the basis of the findings, the use of antibodies that block additional members of the immune checkpoint family, such as TIGIT, may have therapeutic potential in patients with lymphoma. Clinical trials (NCT02794571, NCT02913313, NCT03119428, NCT02964013, NCT03628677) are therefore investigating the efficacy of TIGIT blockade in patients with cancer.

In summary, the current study found that TIGIT was expressed on the majority of intratumoral T cells in follicular lymphoma including T_{reg}, T_{FH}, and exhausted T cells. $TIGIT^+$ T cells showed reduced cytokine production and poor proliferative capacity, and displayed a distinct phenotype compared to $TIGIT^-$ T cells. Clinically, increased numbers of $TIGIT^+$ T cells are associated with an inferior survival in follicular lymphoma and anti–PD-1 therapy has differential effect on TIGIT subsets. Taken together, by utilizing high-throughput technology and comprehensive analysis of a large patient cohort, the current study provides a greater understanding of the biological and clinical roles of TIGIT, and also supports the therapeutic potential of targeting TIGIT in follicular lymphoma.

Disclosure of Potential Conflicts of Interest

Z.-Z. Yang reports grants from NIH, Jaime Erin Follicular Lymphoma Consortium, Leukemia & Lymphoma Society, and Predolin Foundation during the conduct of the study. W. Ding reports grants from Merck (research support for the clinical trial to institution) during the conduct of the study, as well as research funding from Octapharma, Alexion, MEI pharma (advisory board, fee directed to institution) outside the submitted work. A.J. Novak reports research funding from Celgene/BMS (research collaboration) outside the submitted work. S.M. Ansell reports research funding for clinical trials from BMS, Affirmed, Trillium, Seattle Genetics, ADC Therapeutics, and Regeneron during the conduct of the study. No potential conflicts of interest were disclosed by the other authors.

Authors' Contributions

Z.-Z. Yang: Conceptualization, resources, data curation, software, formal analysis, supervision, validation, investigation, visualization, methodology, writing-original draft, project administration, writing-review and editing. **H.J. Kim:** Data curation, investigation, methodology. **H. Wu:** Data curation, software, investigation, methodology. **S. Jalali:** Data curation, investigation, writing-review and editing. **X. Tang:** Data curation, investigation. **J.E. Krull:** Formal analysis, investigation, methodology. **W. Ding:** Supervision, investigation, project administration. **A.J. Novak:** Resources, project administration, writing-review and editing. **S.M. Ansell:** Conceptualization, resources, formal analysis, supervision, funding acquisition, investigation, writing-original draft, project administration, writing-review and editing.

Acknowledgments

This work was supported in part by grants from the NIH (P50 CA97274), the Jaime Erin Follicular Lymphoma Consortium, and the Leukemia & Lymphoma Society and the Predolin Foundation.

The costs of publication of this article were defrayed in part by the payment of page charges. This article must therefore be hereby marked *advertisement* in accordance with 18 U.S.C. Section 1734 solely to indicate this fact.

Received February 11, 2020; revised June 1, 2020; accepted June 30, 2020; published first July 6, 2020.

References

1. Yu X, Harden K, Gonzalez LC, Francesco M, Chiang E, Irving B, et al. The surface protein TIGIT suppresses T cell activation by promoting the generation of mature immunoregulatory dendritic cells. Nat Immunol 2009;10:48–57.
2. Stanietsky N, Simic H, Arapovic J, Toporik A, Levy O, Novik A, et al. The interaction of TIGIT with PVR and PVRL2 inhibits human NK cell cytotoxicity. Proc Natl Acad Sci U S A 2009;106:17858–63.
3. Boles KS, Vermi W, Facchetti F, Fuchs A, Wilson TJ, Diacovo TG, et al. A novel molecular interaction for the adhesion of follicular CD4 T cells to follicular DC. Eur J Immunol 2009;39:695–703.
4. Joller N, Hafler JP, Brynedal B, Kassam N, Spoerl S, Levin SD, et al. Cutting edge: TIGIT has T cell-intrinsic inhibitory functions. J Immunol 2011;186:1338–42.
5. Stengel KF, Harden-Bowles K, Yu X, Rouge L, Yin J, Comps-Agrar L, et al. Structure of TIGIT immunoreceptor bound to poliovirus receptor reveals a cell-cell adhesion and signaling mechanism that requires cis-trans receptor clustering. Proc Natl Acad Sci U S A 2012;109:5399–404.
6. Kurtulus S, Sakuishi K, Ngiow SF, Joller N, Tan DJ, Teng MW, et al. TIGIT predominantly regulates the immune response via regulatory T cells. J Clin Invest 2015;125:4053–62.
7. Chauvin JM, Pagliano O, Fourcade J, Sun Z, Wang H, Sander C, et al. TIGIT and PD-1 impair tumor antigen-specific CD8(+) T cells in melanoma patients. J Clin Invest 2015;125:2046–58.
8. Johnston RJ, Comps-Agrar L, Hackney J, Yu X, Huseni M, Yang Y, et al. The immunoreceptor TIGIT regulates antitumor and antiviral CD8(+) T cell effector function. Cancer Cell 2014;26:923–37.
9. Kong Y, Zhu L, Schell TD, Zhang J, Claxton DF, Ehmann WC, et al. T-cell immunoglobulin and ITIM domain (TIGIT) associates with CD8+ T-cell exhaustion and poor clinical outcome in AML patients. Clin Cancer Res 2016;22:3057–66.
10. Catakovic K, Gassner FJ, Ratswohl C, Zaborsky N, Rebhandl S, Schubert M, et al. TIGIT expressing CD4+T cells represent a tumor-supportive T cell subset in chronic lymphocytic leukemia. Oncoimmunology 2017;7:e1371399.
11. Jariwala N, Benoit B, Kossenkov AV, Oetjen LK, Whelan TM, Cornejo CM, et al. TIGIT and helios are highly expressed on CD4(+) T cells in sezary syndrome patients. J Invest Dermatol 2017;137:257–60.
12. Guillerey C, Harjunpaa H, Carrie N, Kassem S, Teo T, Miles K, et al. TIGIT immune checkpoint blockade restores CD8(+) T-cell immunity against multiple myeloma. Blood 2018;132:1689–94.
13. Tassi E, Grazia G, Vegetti C, Bersani I, Bertolini G, Molla A, et al. Early effector T lymphocytes coexpress multiple inhibitory receptors in primary non-small cell lung cancer. Cancer Res 2017;77:851–61.
14. Josefsson SE, Huse K, Kolstad A, Beiske K, Pende D, Steen CB, et al. T cells expressing checkpoint receptor TIGIT are enriched in follicular lymphoma tumors and characterized by reversible suppression of T-cell receptor signaling. Clin Cancer Res 2018;24:870–81.
15. Josefsson SE, Beiske K, Blaker YN, Forsund MS, Holte H, Ostenstad B, et al. TIGIT and PD-1 mark intratumoral T cells with reduced effector function in B-cell non-hodgkin lymphoma. Cancer Immunol Res 2019;7:355–62.
16. Yang ZZ, Kim HJ, Villasboas JC, Chen YP, Price-Troska T, Jalali S, et al. Expression of LAG-3 defines exhaustion of intratumoral PD-1+ T cells and correlates with poor outcome in follicular lymphoma. Oncotarget 2017;8:61425–39.
17. Kotecha N, Krutzik PO, Irish JM. Web-based analysis and publication of flow cytometry experiments. Curr Protoc Cytom 2010;Chapter 10:Unit10.17.
18. Yang ZZ, Kim HJ, Villasboas JC, Price-Troska T, Jalali S, Wu H, et al. Mass cytometry analysis reveals that specific intratumoral CD4(+) T cell subsets correlate with patient survival in follicular lymphoma. Cell Rep 2019;26:2178–93 e3.
19. Miyara M, Yoshioka Y, Kitoh A, Shima T, Wing K, Niwa A, et al. Functional delineation and differentiation dynamics of human CD4+ T cells expressing the FoxP3 transcription factor. Immunity 2009;30:899–911.
20. Imanguli MM, Cowen EW, Rose J, Dhamala S, Swaim W, Lafond S, et al. Comparative analysis of FoxP3(+) regulatory T cells in the target tissues and blood in chronic graft versus host disease. Leukemia 2014;28:2016–27.
21. Dave SS, Wright G, Tan B, Rosenwald A, Gascoyne RD, Chan WC, et al. Prediction of survival in follicular lymphoma based on molecular features of tumor-infiltrating immune cells. N Engl J Med 2004;351:2159–69.
22. Glas AM, Knoops L, Delahaye L, Kersten MJ, Kibbelaar RE, Wessels LA, et al. Gene-expression and immunohistochemical study of specific T-cell subsets and accessory cell types in the transformation and prognosis of follicular lymphoma. J Clin Oncol 2007;25:390–8.
23. Alvaro T, Lejeune M, Salvado MT, Lopez C, Jaen J, Bosch R, et al. Immunohistochemical patterns of reactive microenvironment are associated with clinicobiologic behavior in follicular lymphoma patients. J Clin Oncol 2006;24:5350–7.
24. de Jong D, Koster A, Hagenbeek A, Raemaekers J, Veldhuizen D, Heisterkamp S, et al. Impact of the tumor microenvironment on prognosis in follicular lymphoma is dependent on specific treatment protocols. Haematologica 2009;94:70–7.
25. Canioni D, Salles G, Mounier N, Brousse N, Keuppens M, Morchhauser F, et al. High numbers of tumor-associated macrophages have an adverse prognostic value that can be circumvented by rituximab in patients with follicular lymphoma enrolled onto the GELA-GOELAMS FL-2000 trial. J Clin Oncol 2008;26:440–6.
26. Xiu B, Lin Y, Grote DM, Ziesmer SC, Gustafson MP, Maas ML, et al. IL-10 induces the development of immunosuppressive CD14(+)HLA-DR(low/-) monocytes in B-cell non-Hodgkin lymphoma. Blood Cancer J 2015;5:e328.
27. Smeltzer JP, Jones JM, Ziesmer SC, Grote DM, Xiu B, Ristow KM, et al. Pattern of CD14+ follicular dendritic cells and PD1+ T cells independently predicts time to transformation in follicular lymphoma. Clin Cancer Res 2014;20:2862–72.
28. Farinha P, Masoudi H, Skinnider BF, Shumansky K, Spinelli JJ, Gill K, et al. Analysis of multiple biomarkers shows that lymphoma-associated macrophage (LAM) content is an independent predictor of survival in follicular lymphoma (FL). Blood 2005;106:2169–74.
29. Chen YP, Kim HJ, Wu H, Price-Troska T, Villasboas JC, Jalali S, et al. SIRPalpha expression delineates subsets of intratumoral monocyte/macrophages with different functional and prognostic impact in follicular lymphoma. Blood Cancer J 2019;9:84.
30. Kridel R, Xerri L, Gelas-Dore B, Tan K, Feugier P, Vawda A, et al. The prognostic impact of CD163-positive macrophages in follicular lymphoma: a study from the BC cancer agency and the lymphoma study association. Clin Cancer Res 2015;21:3428–35.
31. Yang ZZ, Grote DM, Ziesmer SC, Xiu B, Novak AJ, Ansell SM. PD-1 expression defines two distinct T-cell sub-populations in follicular lymphoma that differentially impact patient survival. Blood Cancer J 2015;5:e281.
32. Yang ZZ, Grote DM, Ziesmer SC, Niki T, Hirashima M, Novak AJ, et al. IL-12 upregulates TIM-3 expression and induces T cell exhaustion in patients with follicular B cell non-Hodgkin lymphoma. J Clin Invest 2012;122:1271–82.
33. Lesokhin AM, Ansell SM, Armand P, Scott EC, Halwani A, Gutierrez M, et al. Nivolumab in patients with relapsed or refractory hematologic malignancy: preliminary results of a phase Ib study. J Clin Oncol 2016;34:2698–704.
34. Bin Dhuban K, d'Hennezel E, Nashi E, Bar-Or A, Rieder S, Shevach EM, et al. Coexpression of TIGIT and FCRL3 identifies Helios+ human memory regulatory T cells. J Immunol 2015;194:3687–96.
35. Fuhrman CA, Yeh WI, Seay HR, Saikumar Lakshmi P, Chopra G, Zhang L, et al. Divergent phenotypes of human regulatory T cells expressing the receptors TIGIT and CD226. J Immunol 2015;195:145–55.
36. Raimondi G, Shufesky WJ, Tokita D, Morelli AE, Thomson AW. Regulated compartmentalization of programmed cell death-1 discriminates CD4+CD25+ resting regulatory T cells from activated T cells. J Immunol 2006;176:2808–16.
37. Lucca LE, Axisa PP, Singer ER, Nolan NM, Dominguez-Villar M, Hafler DA. TIGIT signaling restores suppressor function of Th1 tregs. JCI Insight 2019;4:e124427.
38. Wu L, Mao L, Liu JF, Chen L, Yu GT, Yang LL, et al. Blockade of TIGIT/CD155 signaling reverses T-cell exhaustion and enhances antitumor capability in head and neck squamous cell carcinoma. Cancer Immunol Res 2019;7:1700–13.
39. Blake SJ, Dougall WC, Miles JJ, Teng MW, Smyth MJ. Molecular pathways: targeting CD96 and TIGIT for cancer immunotherapy. Clin Cancer Res 2016;22:5183–8.
40. He W, Zhang H, Han F, Chen X, Lin R, Wang W, et al. CD155T/TIGIT signaling regulates CD8(+) T-cell metabolism and promotes tumor progression in human gastric cancer. Cancer Res 2017;77:6375–88.
41. Yang ZZ, Novak AJ, Ziesmer SC, Witzig TE, Ansell SM. Malignant B cells skew the balance of regulatory T cells and TH17 cells in B-cell non-Hodgkin's lymphoma. Cancer Res 2009;69:5522–30.
42. Strioga M, Pasukoniene V, Characiejus D. CD8+ CD28- and CD8+ CD57+ T cells and their role in health and disease. Immunology 2011;134:17–32.
43. Kern F, Khatamzas E, Surel I, Frommel C, Reinke P, Waldrop SL, et al. Distribution of human CMV-specific memory T cells among the CD8pos.

subsets defined by CD57, CD27, and CD45 isoforms. Eur J Immunol 1999;29: 2908–15.
44. Pangrazzi L, Reidla J, Arana JAC, Naismith E, Miggitsch C, Meryk A, et al. CD28 and CD57 define four populations with distinct phenotypic properties within human CD8(+) T cells. Eur J Immunol 2019;50: 363–79.
45. Hung AL, Maxwell R, Theodros D, Belcaid Z, Mathios D, Luksik AS, et al. TIGIT and PD-1 dual checkpoint blockade enhances antitumor immunity and survival in GBM. Oncoimmunology 2018;7:e1466769.
46. Liu X, Li M, Wang X, Dang Z, Jiang Y, Wang X, et al. PD-1(+) TIGIT(+) CD8 (+) T cells are associated with pathogenesis and progression of patients with hepatitis B virus-related hepatocellular carcinoma. Cancer Immunol Immunother 2019;68:2041–54.
47. Kamphorst AO, Wieland A, Nasti T, Yang S, Zhang R, Barber DL, et al. Rescue of exhausted CD8 T cells by PD-1-targeted therapies is CD28-dependent. Science 2017;355:1423–7.
48. Hui E, Cheung J, Zhu J, Su X, Taylor MJ, Wallweber HA, et al. T cell costimulatory receptor CD28 is a primary target for PD-1-mediated inhibition. Science 2017;355:1428–33.
49. Dixon KO, Schorer M, Nevin J, Etminan Y, Amoozgar Z, Kondo T, et al. Functional anti-TIGIT antibodies regulate development of autoimmunity and antitumor immunity. J Immunol 2018;200:3000–7.